Journal of Marine Science and Application (2024) 23: 867-876
https://doi.org/10.1007/s11804-024-00543-x

RESEARCH ARTICLE

Wave Response to a Non-uniform Porous Vertical Plate

Shreya Banerjee[1], Dibakar Mondal[2] and Sudeshna Banerjea[1]

Received: 31 January 2024 / Accepted: 23 May 2024

Abstract

This paper is concerned with a study of wave propagation due to scattering of an obliquely incident wave by a porous vertical plate with non-uniform porosity which is completely submerged in water of finite depth. The problem is formulated in terms of a Fredholm integral equation of the second kind in difference in potential across the barrier. The integral equation is then solved using two methods: the boundary element method and the collocation method. The reflection coefficients, transmission coefficient, and amount of energy dissipation are evaluated using the solution of the integral equation. It is observed that non-uniform porosity of a barrier has significant effect on the reflection of waves and energy dissipation compared to a barrier with uniform porosity. The dissipation of the wave energy by a non-uniform porous barrier can be enhanced and can be made larger than that of a barrier with uniform porosity, by suitable choice of non-uniform porosity distribution in the barrier. This has an important bearing on reducing the wave power and thereby protecting the shore line from coastal erosion. Also, an obliquely incident wave reduces reflection and dissipation while increasing transmission of wave energy as compared to a normally incident wave.

Keywords Vertical plate; Oblique incidence; Finite depth; Non-uniform porosity; Reflection coefficient; Transmission coefficient; Energy dissipation

1 Introduction

A study of wave interaction with porous coastal structures like rubble mound breakwaters became important in coastal engineering during the latter half of the 20th century because of the reason that the structural voids in the porous breakwaters can dissipate wave energy efficiently. Due to this advantage of porosity, the porous breakwaters are preferred over rigid breakwaters as the rigid structures cannot withstand the huge wave load and collapse subsequently.

The literature on the problem of oblique wave diffraction by a rigid vertical barrier in finite-depth water is quite adequate. Many researchers used various methods to study this class of problems. Goswami (1983) employed a singular integral equation formulation based on Green's integral theorem to study the oblique wave scattering problem involving a fixed, vertical, rigid plate submerged in uniform, finite-depth water. Losada et al. (1992) obtained the reflection and transmission coefficients of the above-mentioned problem by using an eigenfunction expansion method. Later on, Porter and Evans (1995) used an approximate method based on the multi-term Galerkin approximation to study oblique wave scattering by a thin, vertical, rigid barrier in uniform, finite-depth water having four basic configurations: a surface-piercing barrier, a bottom-standing barrier, a barrier with a gap and a totally submerged barrier. Also, Mandal and Dolai (1994) considered oblique water wave scattering by a thin vertical barrier in uniform finite-depth water. They employed a one-term Galerkin approximation to evaluate the upper and lower bounds for the transmission and reflection coefficients.

The phenomena of wave propagation through porous media were studied by Sollitt and Cross (1972). Later Chwang (1983) studied the wavemaker problem and he pioneered in mathematical modelling of porous structure as thin porous vertical wave maker. Many researchers studied the problem of diffraction of water waves by porous breakwaters using Sollitt and Cross's model (1972). Yu (1995) used matched expansion method to study the problem of wave diffraction by a porous breakwater. Sahoo (1998) studied the problems of scattering of surface water waves normally incident on a nearly hard (considering the porosity effect to be very small) partially immersed and bottom standing porous vertical barrier present in the deep ocean. The prob-

Article Highlights

- Wave interaction with a non-uniform porous plate is studied.
- Fredholm integral equation formulation is used.
- Proper choice of non-uniform porosity distribution in the barrier can reduce the wave power.

✉ Sudeshna Banerjea
sudeshna.banerjea@yahoo.co.in

[1] Department of Mathematics, Jadavpur University, Kolkata 700032, India

[2] Department of Mathematics, Government General Degree College at Kalna-I, Muragacha, Medgachi, PurbaBurdwan 713405, India

lem is studied by using perturbation analysis for very small values of the non-dimensional porosity parameter. Later Gayen and Mandal (2014) used a second-kind hypersingular integral equation formulation to study the problem of wave diffraction by a submerged porous plate in an ocean with a free surface. Mondal and Banerjea (2016) studied the problem of scattering of water waves by a porous plate submerged in the ocean with ice cover and inclined at an angle α to the vertical using a second-kind hypersingular integral equation formulation. In the literature mentioned above, the porosity of the plate is taken to be uniform. A study of wave interaction with a porous barrier with non-uniform porosity are limited in the literature. Tao et al., (2009) used eigen function expansion method and Song and Tao (2010) adopted numerical method and studied the problem of wave interaction with a perforated cylindrical breakwater with non-uniform porosity. Later, Singh et al. (2022) studied the phenomena of water wave propagation in the presence of an inclined flexible plate with variable porosity using hypersingular integral equation formulation. Gupta and Gayen (2019) and Sarkar et al (2020) studied the problem of wave interaction with dual porous barrier with non-uniform porosity using coupled integral equation formulation. Recently Mondal et al. (2024) studied the effect of non-uniform porosity of a porous vertical barrier on an obliquely incident wave train. They considered two configurations of the barrier, viz, partially immersed and the bottom standing barrier and used Fredholm integral equation formulation to study the problem.

In the present paper, we study the problem of scattering of obliquely incident wave by a porous plate with non-uniform porosity submerged in water of finite depth. Here the problem concerned is formulated in terms of a Fredholm integral equation of the second kind, defined in a single interval, by using an eigen function expansion of the water wave potential (Mondal et al., 2024). The unknown function satisfying the Fredholm integral equation represents the difference of potentials across the barrier. We may mention here that the integral equation here has a regular kernel which is more amenable to the numerical methods. The integral equation is then solved using two methods: the boundary element method and the collocation method. Recently Banerjea et al solved integral equation with regular and singular kernel, numerically by applying boundary element method (Banerjea et al., 2019; Samanta et al., 2022). This is a simple numerical method of solving integral equation with complicated kernel, where the range of integration and the interval of definition of the integral equation are divided into small subintervals (line elements). Assuming the unknown function satisfying the integral equation to be constant in each line element, the integral equation is reduced to a system of algebraic equations. In the collocation method, the unknown function is represented as a series involving Chebychev's polynomials and thereby the integral equation is reduced to a system of algebraic equation(Parsons and Martin, 1992; 1994). The solution of the integral equation is then used to evaluate the reflection coefficient, transmission coefficient and amount of energy dissipated which were then depicted graphically. It is observed that by a proper choice of non-uniform porosity distribution in a barrier, the dissipation of the wave energy due to a barrier with non-uniform porosity, can be made larger than by a barrier with uniform porosity. This is important in reducing the wave power and protecting the shore line from coastal erosion. Also, an obliquely incident wave reduces reflection and dissipation while increasing transmission of wave energy as compared to a normally incident wave.

2 Formulation of the problem

We consider two dimensional irrotational motion in water due to oblique incidence of a time harmonic wave train on a thin vertical porous plate with nonuniform porosity, submerged in water. The water occupies the region $0 < y < h$, where y-axis is vertically downwards and $\boldsymbol{x}$-axis is along the mean free surface. The vertical porous barrier is represented by $x = 0, y \in \mathcal{L}$, where $\mathcal{L} = (a, b)$. A schematic diagram is given in Figure 1.

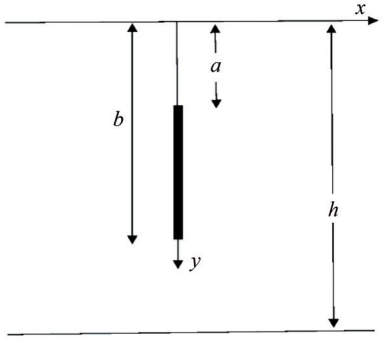

Figure 1 Schematic diagram

A train of progressive waves represented by velocity potential $\mathrm{Re}\left\{\phi^{\mathrm{inc}}(x,y)\mathrm{e}^{iyz-i\sigma t}\right\}$, is incident obliquely at an angle α to the horizontal axis, on the thin vertical barrier. Here σ is the circular frequency, γ is the wave number along the z-direction, $\gamma = k_0 \sin\alpha$, k_0 is the unique positive root of the equation $k\tanh kh = K$, $K = \sigma^2/g$, g is the acceleration due to gravity (Mandal and Chakrabarti, 2000).

Assuming linear theory and describing the resulting motion by the velocity potential $\mathrm{Re}\left\{\phi(x,y)\mathrm{e}^{iyz-i\sigma t}\right\}$, the function ϕ satisfies

$$\left(\nabla^2 - \gamma^2\right)\phi = 0 \text{ in the water region} \tag{1}$$

$$K\phi + \phi_y = 0 \text{ on } y = 0 \tag{2}$$

the boundary condition on the porous barrier $\mathcal{L}$ which is given by

$$\phi_x = -ik_0\lambda(y)[\phi](y) \text{ on } x=0,\ y\epsilon\mathcal{L} \tag{3}$$

Here $[\phi]=\phi^+(0,y)-\phi^-(0,y)$, ϕ^+, ϕ^- are potential functions on the right hand side and left hand side of the barrier $\mathcal{L}$, respectively, and $\lambda(y)=\lambda_r(y)+i\lambda_i(y)$ is the non-uniform porous-effect parameter where $\lambda_r(y)$ is associated with resistance force coefficient and $\lambda_i(y)$ is associated with inertial force coefficient of the porous barrier (Yu, 1995)

$$r^{\frac{1}{2}}\nabla\phi \text{ is bounded as } r\to 0 \tag{4}$$

where $\boldsymbol{r}$ is the distance from a submerged end of the barrier,

$$\phi_y = 0 \text{ on } y=h \tag{5}$$

The far field conditions are given by

$$\phi(x,y)\to\begin{cases} \phi^{\text{inc}}(x,y)+R\phi^{\text{inc}}(-x,y) & \text{as } x\to-\infty,\\ T\phi^{\text{inc}}(x,y) & \text{as } x\to\infty \end{cases} \tag{6}$$

where R and T are the complex reflection and transmission coefficients, respectively, and

$$\phi^{\text{inc}}(x,y)=\frac{g^2}{\sigma^3}\frac{\cosh k_0(h-y)e^{i\mu x}}{\cosh k_0 h},\qquad \mu=k_0\cos\alpha$$

Here $k=\pm k_0, \pm ik_n$, $n=1,2,\cdots$ are the roots of

$$k\tanh kh - K = 0 \tag{7}$$

3 Method of solution

Applying Havelock's expansion of the velocity potential an appropriate eigen functions expansion of $\phi(x,y)$ is given by

$$\phi(x,y)\to\begin{cases} T\phi^{\text{inc}}(x,y)+\sum_{n=1}^{\infty}\mathcal{A}_n\cos k_n(h-y)e^{-s_nx},\ x>0\\ \phi^{\text{inc}}(x,y)+R\phi^{\text{inc}}(-x,y)+\sum_{n=1}^{\infty}\mathcal{B}_n\cos k_n(h-y)e^{s_nx},\ x<0 \end{cases} \tag{8}$$

where $s_n^2=k_n^2+\gamma^2$.

Let

$$F(y)=\phi_x(0,y),\ 0<y<h. \tag{9}$$

and

$$G(y)=\phi(0^+,y)-\phi(0^-,y),\ 0<y<h \tag{10}$$

So that equation (3) yields

$$F(y)=-ik_0\lambda(y)G(y) \text{ for } y\epsilon\mathcal{L} \tag{11}$$

and

$$G(y)=0 \text{ for } y\epsilon\bar{\mathcal{L}} \tag{12}$$

where $\bar{\mathcal{L}}=(0,h)\backslash\mathcal{L}$.

Using relation (8) in equations (9) we have for $0<y<h$,

$$\begin{aligned} F(y)&=i\mu T\frac{g^2}{\sigma^3}\frac{\cosh k_0(h-y)}{\cosh k_0 h}-\sum_{n=1}^{\infty}\mathcal{A}_n s_n\cos k_n(h-y)\\ &=i\mu(1-R)\frac{g^2}{\sigma^3}\frac{\cosh k_0(h-y)}{\cosh k_0 h}+\sum_{n=1}^{\infty}\mathcal{B}_n s_n\cos k_n(h-y) \end{aligned} \tag{13}$$

The relation (13) shows that

$$T=1-R,\ \mathcal{A}_n=-\mathcal{B}_n \tag{14}$$

By Havelock's inversion theorem we obtain from equations (13) after using relations (11) and (12),

$$1-R=\frac{\sigma^3}{g^2}\frac{4k_0\cosh k_0 h}{i\mu(2k_0h+\sinh 2k_0h)}\left[-ik_0\int_{\mathcal{L}}\lambda(y)G(y)\cosh k_0(h-y)dy+\int_{\bar{\mathcal{L}}}F(y)\cosh k_0(h-y)\mathrm{d}y\right] \tag{15}$$

$$\mathcal{A}_n=\frac{-4k_n}{s_n(2k_nh+\sin 2k_nh)}\left[-ik_0\int_{\mathcal{L}}\lambda(y)G(y)\cos k_n(h-y)\mathrm{d}y+\int_{\bar{\mathcal{L}}}F(y)\cos k_n(h-y)\mathrm{d}y\right] \tag{16}$$

Again using equation (8) in equation (10) and noting equation (14) we have,

$$G(y)=-2R\frac{g^2}{\sigma^3}\frac{\cosh k_0(h-y)}{\cosh k_0 h}+2\sum_{n=1}^{\infty}\mathcal{A}_n\cos k_n(h-y),\quad 0<y<h \tag{17}$$

Applying Havelock's inversion formula to equation (17),

we get

$$R = \frac{\sigma^3}{g^2}\frac{-2k_0\cosh k_0h}{(2k_0h+\sinh 2k_0h)}\int_{\mathcal{L}} G(y)\cosh k_0(h-y)\mathrm{d}y \quad (18)$$

$$\mathcal{A}_n = \frac{2k_n}{(2k_nh+\sin 2k_nh)}\int_{\mathcal{L}} G(y)\cos k_n(h-y)\mathrm{d}y \quad (19)$$

After using equations (13) and (19) in equation (11) a Fredholm integral equation of second kind (Mikhlin, 1957) for $G(y)$ is obtained as

$$\frac{ik_0\lambda(y)G(y)}{2} + \frac{i\mu(1-R)}{2}\frac{g^2}{\sigma^3}\frac{\cosh k_0(h-y)}{\cosh k_0h} = \frac{\cosh^2 k_0h}{(2k_0h+\sinh 2k_0h)}\int_{\mathcal{L}} G(u)\mathcal{K}(y,u)\mathrm{d}u, y\epsilon\mathcal{L} \quad (20)$$

where

$$\mathcal{K}(y,u) = \frac{(2k_0h+\sinh 2k_0h)}{\cosh^2 k_0h}\lim_{\varepsilon\to 0}\sum_{n=1}^{\infty}\frac{s_nk_n\cos k_n(h-u)\cos k_n(h-y)}{(2k_nh+\sin 2k_nh)}e^{-\varepsilon k_n} \quad (21)$$

Here we introduced the exponential term to ensure the convergency of the series.

Defining

$$\mathcal{G}_0(y) = \frac{\sigma^3}{g^2}\frac{2G(y)}{i(1-R)} \quad (22)$$

the integral equation (20) is alternatively written as

$$\frac{2\cosh^2 k_0h}{(2k_0h+\sinh 2k_0h)}\int_{\mathcal{L}}\mathcal{G}_0(u)\mathcal{K}(y,u)\mathrm{d}u - ik_0\lambda(y)\mathcal{G}_0(y) = \frac{2\mu\cosh k_0(h-y)}{\cosh k_0h}, y\epsilon\mathcal{L} \quad (23)$$

Using the relations (18) and (22) we write

$$R = \frac{\mathcal{D}}{1+\mathcal{D}} \quad (24)$$

where

$$\mathcal{D} = \frac{k_0\cosh k_0h}{i(2k_0h+\sinh 2k_0h)}\int_{\mathcal{L}}\mathcal{G}_0(y)\cosh k_0(h-y)\mathrm{d}y \quad (25)$$

The equations (24) and (25), give a relation between R and the unknown function $\mathcal{G}_0(y)$.

Thus solving the integral equation (23) the unknown function $\mathcal{G}_0(y)$ can be obtained and using $\mathcal{G}_0(y)$ in relations (24) and (25), the reflection coefficient R can be evaluated.

Substituting $y = \frac{b+a}{2}+\frac{b-a}{2}s$ and $u = \frac{b+a}{2}+\frac{b-a}{2}t$ in the integral equation (23), it reduces to

$$-ik_0\lambda_1(s)\mathcal{G}_1(s) + (b-a)\int_{-1}^{1}\mathcal{G}_1(t)\mathcal{K}_1(s,t)\mathrm{d}t = \frac{2\mu\cosh k_0\left(\frac{(2h-a-b)-(b-a)s}{2}\right)}{\cosh k_0h}, -1<s<1 \quad (26)$$

where

$$\mathcal{G}_0\left(\frac{b+a}{2}+\frac{b-a}{2}t\right) = \mathcal{G}_1(t), \lambda\left(\frac{b+a}{2}+\frac{b-a}{2}s\right) = \lambda_1(s), \quad s_n^2 = k_n^2 + k_0^2\sin^2\alpha$$

and

$$\mathcal{K}_1(s,t) = \sum_{n=1}^{\infty}\frac{s_nk_n\cos k_n\left(\frac{(2h-a-b)-(b-a)t}{2}\right)\cos k_n\left(\frac{(2h-a-b)-(b-a)s}{2}\right)}{(2k_nh+\sin 2k_nh)}$$

We may note that the integral equation (26) is a regular integral equation, which can be solved by using two different methods below:

Method I: Collocation method

In this method, the unknown function $\mathcal{G}_1(t)$ is approximated as(Parsons and Martin, 1992; 1994)

$$\mathcal{G}_1(t) = \sqrt{1-t^2}\sum_{n=0}^{N}p_nU_n(t), \quad (27)$$

where $U_n(t)$are Chebychev polynomial of second kind, $p_n(n=0,1,2,\cdots,N)$are unknown constants to be found.

Thus the integral equation (26) reduces to the following system of linear algebraic equations in p_n.

$$\sum_{i=0}^{N}\mathcal{C}_i(s)\,p_i = \mathcal{X}(s) \quad (28)$$

where

$$\mathcal{C}_i(s) = (b-a)\sum_{n=1}^{\infty}\left\{\frac{\sqrt{k_n^2 + k_0^2\sin^2\alpha}\, k_n \cos k_n\left(\frac{(2h-a-b)-(b-a)s}{2}\right)}{\left(2k_n h + \sin 2k_n h\right)}\int_{-1}^{1}\sqrt{1-t^2}\cos k_n\left(\frac{(2h-a-b)-(b-a)t}{2}\right)U_i(t)\,\mathrm{d}t\right\}$$
$$-ik_0\lambda_1(s)\sqrt{1-s^2}\,U_i(s)$$

and

$$\mathcal{X}(s) = \frac{2k_0\cos\alpha\cosh k_0\left(\frac{(2h-a-b)-(b-a)s}{2}\right)}{\cosh k_0 h}$$

Choosing the collocation points $s = s_j'$ s in (27) as

$$s_j = \cos\frac{2j+1}{2N+2}\pi,\ j = 0, 1, 2, \cdots, N \tag{29}$$

the system of linear equations (28) reduces to

$$\sum_{i=0}^{N}\mathcal{C}_i\left(s_j\right)p_i = \mathcal{X}\left(s_j\right),\ j = 0, 1, 2, \cdots, N \tag{30}$$

Solving this system of linear equations (30), the constants $p_0, p_1, \cdots, p_N$ can be determined so that $\mathcal{G}_1(t)$, i.e., $\mathcal{G}_0(t)$ can be obtained from equation (27) and hence R from relations (24) and (25).

Method II: Boundary element method

Here, we approximate $\mathcal{G}_1(t)$ as

$$\mathcal{G}_1(t) = \sqrt{1-t^2}\,\mathcal{U}(t) \tag{31}$$

where $\mathcal{U}(t)$ is a regular function in $[-1, 1]$. The square root factors in equation (31) ensures that $\mathcal{G}_1(t)$ has the correct behaviour at the ends of the porous barrier. With this approximation, the integral equation (26) reduces to

$$-ik_0\lambda_1(s)\sqrt{1-s^2}\,\mathcal{U}(s) + (b-a)\int_{-1}^{1}\sqrt{1-t^2}\,\mathcal{U}(t)\mathcal{K}_1(s,t)\,\mathrm{d}t = \frac{2k_0\cos\alpha\cosh k_0\left(\frac{(2h-a-b)-(b-a)s}{2}\right)}{\cosh k_0 h} \tag{32}$$

Now, we divide the domain of the integration $[-1, 1]$ into m number of line elements as $[-1, 1] = \cup_{j=1}^{m}\left[a_{j-1} - a_j\right]$, with end points $a_0 = -1$, $a_m = 1$ and $a_j = a_0 + jr'$ where $r' = \frac{a_m - a_0}{m}$.

Writing $t = t\_j$ for $t\_j \epsilon \left[a\_j - 1, a\_j\right]$,
$t_j = (1-\tau)\,a_{j-1} + \tau a_j$,
where $0 < \tau < 1$, $j = 1, 2, \cdots, m$
and $s = s_i$ for $s_i \epsilon \left[a_{i-1} - a_i\right]$, i.e.,
$s_i = (1-\gamma)\,a_{i-1} + \gamma a_i$,
where $0 < \gamma < 1$, $i = 1, 2, \cdots, m$ (33)

the equation (32) can be alternatively written as

$$\sum_{j=1}^{m}(b-a)\int_0^1\sqrt{1-t_j^2}\,\mathcal{U}\left(t_j\right)\mathcal{K}_1\left(s_i,t_j\right)r'\mathrm{d}\tau - ik_0\lambda_1\left(s_i\right)\sqrt{1-s_i^2}\,\mathcal{U}\left(s_i\right) = \mathcal{X}\left(s_i\right),\ \ i = 1, 2, \cdots, m \tag{34}$$

Now, according to boundary element method approximation, we assume the unknown function in integral equation takes constant values in each small interval, i. e., we take $\mathcal{U}\left(t_j\right) = \mathcal{U}_j$ $j = 1, 2, \cdots, m$ as a constant for jth line element. Thus, the integral equation (34) is reduced to a system of linear equations.

$$\sum_{j=1}^{m}\mathcal{B}_{ij}\mathcal{U}_j = \mathcal{X}\left(s_i\right),\ \ i = 1, 2, \cdots, m \tag{35}$$

where

$$\mathcal{B}_{ij} = \frac{2(b-a)}{m}\sum_{n=1}^{\infty}\left\{\frac{\sqrt{k_n^2 + k_0^2\sin^2\alpha}\, k_n \cos k_n\left(\frac{(2h-a-b)-(b-a)s_i}{2}\right)}{2k_n h + \sin 2k_n h}\int_0^1\sqrt{1-t_j^2}\cos k_n\left(\frac{(2h-a-b)-(b-a)t_j}{2}\right)\mathrm{d}\tau\right\}$$
$$-ik_0\lambda\left(s_i\right)\sqrt{1-s_i^2}\,\delta_{ij}$$

and

$$\mathcal{X}\left(s_i\right) = \frac{2k_0\cos\alpha\cos h\, k_0\left(\frac{(2h-a-b)-(b-a)s_i}{2}\right)}{\cosh k_0 h}$$

Here δ_{ij} is Kronecker delta and

$$\mathcal{U}_j = \mathcal{U}\left(t_j\right),\ j = 1, 2, \cdots, m$$

Now, solving the system of linear equation (35), we obtain

the unknown function $\mathcal{U}_j$ for $j = 1, 2, \cdots, m$, and $\mathcal{G}_1(t_j)$ is approximated in each line intervals to evaluate R.

4 The energy identity

Porosity of the porous barrier causes the dissipation of wave energy, in which case $|R|^2 + |T|^2 < 1$.

We apply Green's theorem to the functions ϕ and $\bar{\phi}$ in the region bounded by the lines $y = 0, -X \leqslant x \leqslant X$; $x = -X, 0 \leqslant y \leqslant h$; $y = h, -X \leqslant x \leqslant X$; $x = X, 0 \leqslant y \leqslant h$ and a contour enclosing the barrier $\mathcal{L}$.

Taking $X \to \infty$, we have

$$|R|^2 + |T|^2 = 1 - J$$

where

$$J = \frac{4k_0 \cosh^2 k_0 h}{\cos\alpha(2k_0 h + \sin \mathrm{h}\, 2k_0 h)} \int_{\mathcal{L}} \lambda_r(y) \left| G(y) \right|^2 \mathrm{d}y \quad (36)$$

J is positive, so $|R|^2 + |T|^2 < 1$, J represents the amount of the dissipation of wave energy.

5 Numerical results

The reflection coefficient $|R|$ the transmission coefficient $|T|$ and the amount of wave energy dissipated J for different forms of porosity distribution function $\lambda(s) = \lambda_r(s) + i\lambda_i(s)$, $-1 \leqslant s \leqslant 1$ can be computed numerically from (24), (25) and (36), respectively, once $\mathcal{G}_0$ are known by solving the integral equations (25) and (26). We may mention here that the porosity distribution function $\lambda(s)$ can be chosen in any suitable form.

However in the present discussion we have analysed the behaviour of $|R|, |T|, J$ for $\lambda(s) = \left\{0, 1, 1 + \frac{i}{2}, \frac{(1+s)}{2}, s^2, 8s^2, \frac{(1+s)\left(1+\frac{i}{2}\right)}{2}, s^2\left(1+\frac{i}{2}\right), -1 < s < 1\right\}$ Separate analysis has to be carried out for any other type of porosity distribution.

I) When $\lambda(s) = \frac{(1+s)}{2}$ then $\lambda_i(s) = 0$ and $\lambda_r(s) = \frac{(1+s)}{2}$ is a linear function of s. So $\lambda_r(s)$ is zero at $s = -1$, i.e., at one end of the barrier and increases as s increases till it reaches a maximum value $\lambda_r(1) = 1$ at the other end of the barrier. Similarly for $\lambda(s) = \frac{(1+s)\left(1+\frac{i}{2}\right)}{2}$, $\lambda_r(s) = \frac{(1+s)}{2}$ and $\lambda_i(s) = \frac{(1+s)}{4}$. In this case $\lambda_r(-1) = \lambda_i(-1) = 0$ and both $\lambda_r(s)$ and $\lambda_i(s)$ increases as $s \to 1$ and both become maximum at the other end of the barrier for which $s = 1$, i.e., $\lambda_r(1) = 1$ and $\lambda_i(1) = \frac{1}{2}$. So when $\lambda(s) = \frac{(1+s)}{2}$, $\frac{(1+s)\left(1+\frac{i}{2}\right)}{2}$, the porosity distribution of the barrier is such that the barrier is rigid at one end and becomes porous towards the ends.

II) For $\lambda(s) = s^2$, $\lambda_i(s) = 0$ and $\lambda_r(s) = s^2$. In this case $\lambda_r(0) = 0$ and $\lambda_r(s)$ increases as $|s|$ increases till it assumes maximum value $\lambda_r(\pm 1) = 1$. Also when $\lambda(s) = s^2\left(1 + \frac{i}{2}\right)$, $\lambda_r(s) = s^2$ and $\lambda_i(s) = \frac{s^2}{2}$. So both $\lambda_r(s)$ and $\lambda_i(s)$ are zero at the center of the barrier and increases as $s \to \pm 1$ till they attain maximum at $s = \pm 1$, i.e., $\lambda_r(\pm 1) = 1$ and $\lambda_i(\pm 1) = \frac{1}{2}$. This shows that the porosity distribution of the barrier for $\lambda(s) = s^2, s^2\left(1 + \frac{i}{2}\right)$ is such that, it is rigid at the centre and porous towards the end.

III) For $\lambda(s) = 8s^2$, $\lambda_i(s) = 0$ and $\lambda_r(s) = 8s^2$. In this case $\lambda_r(0) = 0$ and $\lambda_r(s)$ increases as $|s|$ increases till it assumes maximum value $\lambda_r(\pm 1) = 8$. This shows that the porosity distribution of the barrier for $\lambda(s) = 8s^2$, is such that, it is rigid at the center and porous towards the end. The difference between distribution of porosity in the barrier described in case II) for $\lambda(s) = s^2$ and in III) is that the porosity away from the centre is more for barrier described in III) than for the barrier in case II).

For numerical computation, the value of N in (30) is chosen as $N = 13$ and the value of m in (35) is taken as 60.

In Table 1, $|R|$ for rigid barrier ($\lambda = 0$) obtained by solving integral equation (26) by collocation method and boundary element method are presented for different values of α and for $kh = 0.2$, $\frac{a}{h} = 0.2$, $\frac{b}{h} = 0.6$. It is found that $|R|$ obtained by using both the methods mentioned above agree with each other for three places of decimal. Also the values of $|R|$ are compared with the results obtained by Mandal and Dolai (1994) and it is observed that $|R|$ obtained in the present analysis agrees with the result in (Mandal, Dolai, 1994) up to 3 decimal places. This confirms the correctness of the method used in the present analysis.

Table 1 Reflection coefficient for $Kh = 0.2$; $\frac{a}{h} = 0.2$; $\frac{b}{h} = 0.6$; $\lambda = 0$

α	BEM	Collocation method	Results of mondal and dolai (1994)
0	0.031 5	0.031 8	0.031 8
$\frac{\pi}{6}$	0.027 2	0.027 4	0.027 5
$\frac{\pi}{3}$	0.015 6	0.015 7	0.015 8

Table 2 shows a comparison of the values of $|R|$ obtained from collocation method and boundary element method for a porous barrier with $\lambda = 1 + \frac{i}{2}$ for different values of α and for $Kh = 0.2, \frac{a}{h} = 0.2, \frac{b}{h} = 0.6$. It is observed from Table 2 that values of $|R|$ obtained by solving the integral equation by both methods, agree with each other up to 3 or 4 decimal places. Better accuracy can be achieved by increasing the number of line elements in equation (34) and the number of collocation points N in equation (27).

Table 2 Reflection coefficient for $Kh = 0.2$; $\frac{a}{h} = 0.2$; $\frac{b}{h} = 0.6$; $\lambda = 1 + \frac{i}{2}$

α	BEM	Collocation method
0	0.028 760 1	0.028 836 2
$\frac{\pi}{6}$	0.024 831 5	0.024 898 1
$\frac{\pi}{3}$	0.014 268 2	0.014 307 5

The reflection coefficient $|R|$ and the amount of wave energy dissipated J are computed numerically and depicted graphically against the wave number Kh in the Figures 2–13, for $\frac{a}{h} = 0.2$ and $\frac{b}{h} = \{0.4, 0.6, 0.8\}$ and for various values of the porosity parameter parameter $\lambda(s) = \left\{0, 1, 1 + \frac{i}{2}, \frac{(1+s)}{2}, s^2, 8\,s^2, \frac{(1+s)\left(1+\frac{i}{2}\right)}{2}, s^2\left(1+\frac{i}{2}\right), -1 < s < 1\right\}$, angle of incidence $\alpha = \{0, \pi/3\}$. It is already known that (Yu, 1995) the resistance force coefficient λ_r of the porous material of the barrier resists the passage of water through the pores while the inertial force coefficient λ_i allows the flow through the pores. When the resistance force coefficient λ_r is much greater than the inertial force coefficient λ_i, i.e., $\lambda_r \gg \lambda_i$ then the porosity parameter λ is taken to be real (Yu, 1995).

The energy identity has been verified for rigid barrier, i.e., $\lambda = 0$ and for porous barrier $\lambda \neq 0$.

In Figures 2 to 7, $|R|$ is plotted against wave numbers Kh for various non dimensional parameters, viz, porosity parameter $\lambda \epsilon \left\{0, 1, 1 + \frac{i}{2}, \frac{(1+s)}{2}, s^2, 8\,s^2, \frac{(1+s)\left(1+\frac{i}{2}\right)}{2}, s^2\left(1+\frac{i}{2}\right), -1 < s < 1, \frac{a}{h} = 0.2 \text{ and } \frac{b}{h} \epsilon \{0.4, 0.6, 0.8\}\right.$, angle in incidence $\left.\alpha \epsilon \left\{0, \frac{\pi}{3}\right\}\right\}$.

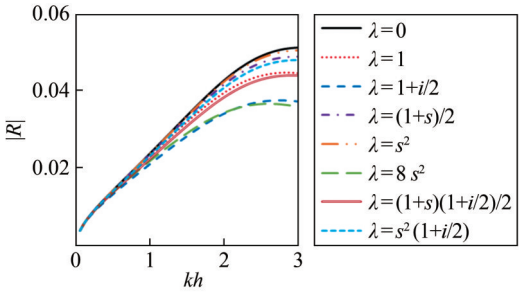

Figure 2 $|R|$ against Kh for $\alpha = 0$, $\frac{a}{h} = 0.2, \frac{b}{h} = 0.4$, for various porosity λ

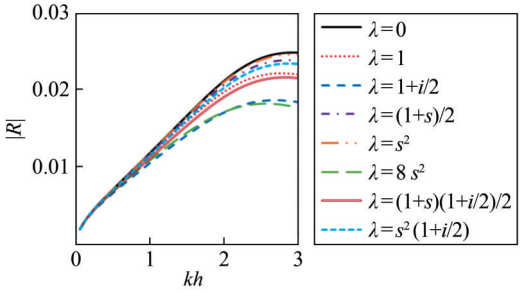

Figure 3 $|R|$ against Kh for $\alpha = \frac{\pi}{3}, \frac{a}{h} = 0.2, \frac{b}{h} = 0.4$, for various porosity λ

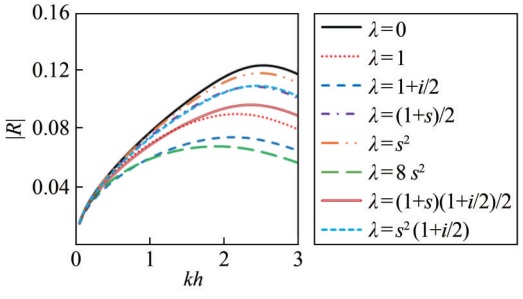

Figure 4 $|R|$ against Kh for $\alpha = 0, \frac{a}{h} = 0.2, \frac{b}{h} = 0.6$, for various porosity λ

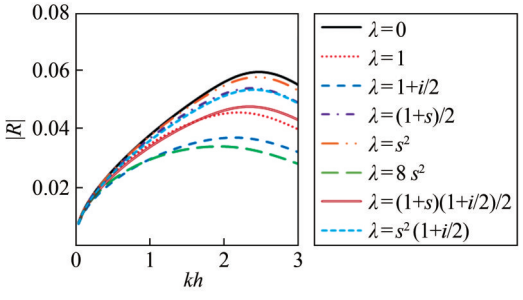

Figure 5 $|R|$ against Kh for $\alpha = \frac{\pi}{3}, \frac{a}{h} = 0.2, \frac{b}{h} = 0.6$, for various porosity λ

The following observations are made from Figures 2–7.

1) From Figures 2 to 7, it is observed that for $\alpha =$

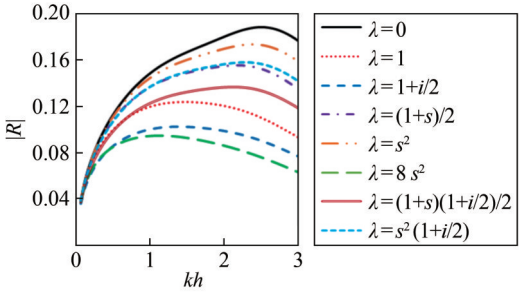

Figure 6 $|R|$ against Kh for $\alpha = 0, \frac{a}{h} = 0.2, \frac{b}{h} = 0.8$, for various porosity λ

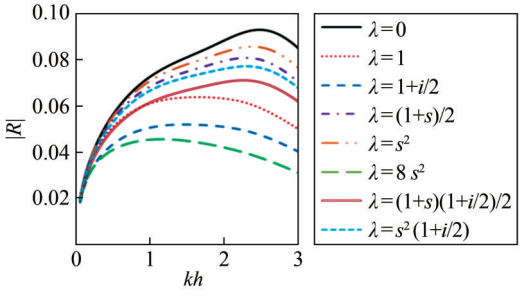

Figure 7 $|R|$ against Kh for $\alpha = \frac{\pi}{3}, \frac{a}{h} = 0.2, \frac{b}{h} = 0.8$, for various porosity λ

$\left\{0, \frac{\pi}{3}\right\}$, $|R|_{\lambda = 8s^2} < |R|_{\lambda = 1} < |R|_{\lambda = \frac{(1+s)}{2}} < |R|_{\lambda = s^2} < |R|_{\lambda = 0}$. Also $|R|_{\lambda = 1 + \frac{i}{2}} < |R|_{\lambda = \frac{(1+s)\left(1+\frac{i}{2}\right)}{2}} < |R|_{\lambda = s^2\left(1+\frac{i}{2}\right)}$. This shows that reflection coefficient for rigid barrier is more than that of porous barrier. Also for the porosity distribution function $\lambda(s)$ chosen in this analysis, it is found that the reflection coefficient $|R|$ depends on the porosity distribution of the barrier. In this study it is seen that maximum reflection of waves occurs for barrier whose porosity distribution is $\lambda = s^2$ and least reflection of waves occurs when $\lambda = 8\,s^2$. Moreover, it is seen from the figures that $|R|$ for $\lambda_i \neq 0$, is less than $|R|$ for $\lambda_i = 0$. This shows that the presence inertial force coefficient in the porosity distribution function allows the passage of water through the pores, and thereby reduces reflection.

2) Comparing Figures 2, 4 and 6 with Figures 3, 5 and 7, it is observed that $|R|_{\alpha = 0} > |R|_{\alpha = \frac{\pi}{3}}$. This shows that the reflection coefficient for a normally incident waves is more than that of an obliquely incident wave.

3) Figures 2 – 7 show that $|R|_{\frac{b}{h} = 0.8} > |R|_{\frac{b}{h} = 0.6} > |R|_{\frac{b}{h} = 0.4}$ from which it can be inferred that long barrier induces more reflection.

In Figures 8–13 the amount of wave energy dissipated J is plotted against the wave number Kh for various values of $\frac{b}{h}$, λ and α. The following observations are made from the Figures 8–13.

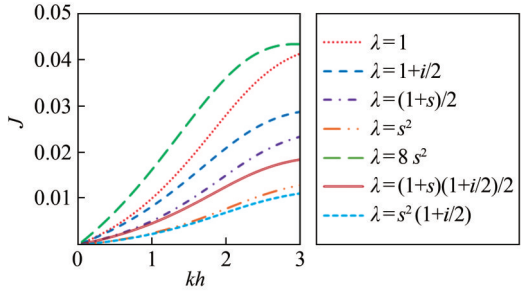

Figure 8 J against Kh for $\alpha = 0, \frac{a}{h} = 0.2, \frac{b}{h} = 0.4$, for various porosity λ

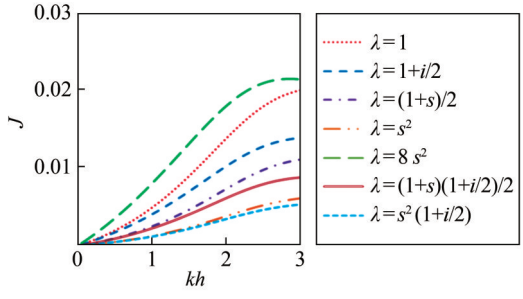

Figure 9 J against Kh for $\alpha = \frac{\pi}{3}, \frac{a}{h} = 0.2, \frac{b}{h} = 0.4$, for various porosity λ

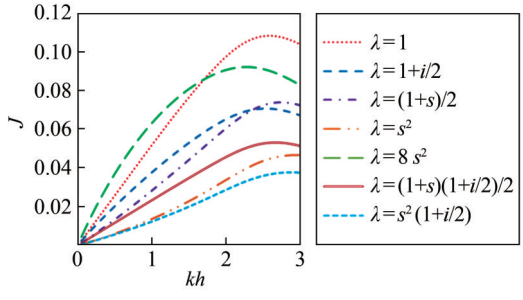

Figure 10 J against Kh for $\alpha = 0, \frac{a}{h} = 0.2, \frac{b}{h} = 0.6$, for various porosity λ

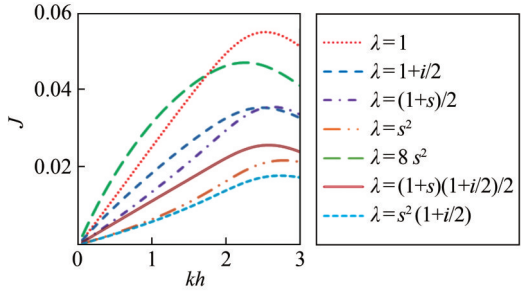

Figure 11 J against Kh for $\alpha = \frac{\pi}{3}, \frac{a}{h} = 0.2, \frac{b}{h} = 0.6$, for various porosity λ

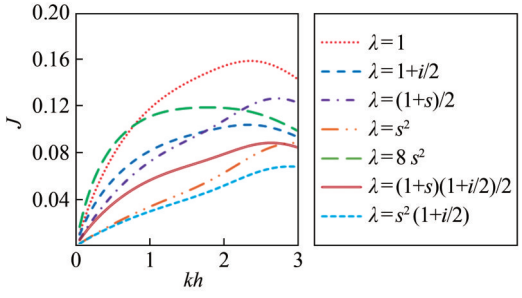

Figure 12 J against Kh for $\alpha = 0, \frac{a}{h} = 0.2, \frac{b}{h} = 0.8$, for various porosity λ

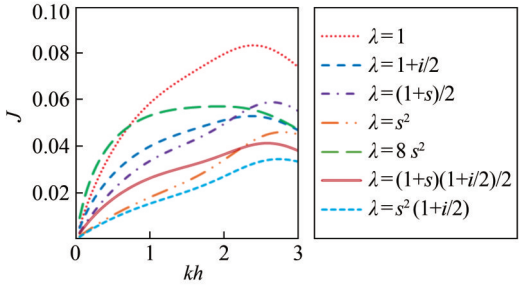

Figure 13 J against Kh for $\alpha = \frac{\pi}{3}, \frac{a}{h} = 0.2, \frac{b}{h} = 0.8$, for various porosity λ

1) It is observed from Figures 8 and 9 that $J_{\lambda=8s^2} > J_{\lambda=1} > J_{\lambda=\frac{(1+s)}{2}} > J_{\lambda=s^2}$ for all Kh when $\frac{a}{h} = 0.2, \frac{b}{h} = 0.4$. This shows that for short barrier, the energy dissipation J is more when $\lambda = 8\,s^2$, than when $\lambda = 1$. This shows that for this particular type of non-uniform porosity distribution, the barrier dissipates more wave energy than a barrier with uniform porosity where $\lambda = 1$. Thus for these choice of porosity distribution, the wave power can be reduced to protect the shore line from the effect of rough sea. However, as the length of the barrier increases, $J_{\lambda=8s^2} > J_{\lambda=1}$ for smaller values of Kh. For larger values of Kh, $J_{\lambda=8s^2} < J_{\lambda=1}$ which shows that energy dissipation of waves with moderate wave length is more for barrier with this type of distribution of non-uniform porosity than for barrier with uniform porosity, i.e., $\lambda = 1$. It is also observed that for any length of the barrier, $J_{\lambda=1+\frac{i}{2}} > J_{\lambda=\frac{(1+s)\left(1+\frac{i}{2}\right)}{2}} > J_{\lambda=s^2\left(1+\frac{i}{2}\right)}$. This shows that energy dissipation for barrier depends on the porosity distribution of the barrier.

2) It is seen that $J_{\lambda_i \neq 0} < J_{\lambda_i = 0}$. This shows that inertial force coefficient of the porous material of the barrier with variable porosity diminishes the energy dissipation.

3) Energy dissipation for obliquely incident wave is less than that of normally incident wave, i.e., $J_{\alpha=0} > J_{\alpha=\frac{\pi}{3}}$

4) For any values of α, λ it is seen that $J_{\frac{b}{h}=0.8} > J_{\frac{b}{h}=0.6} > J_{\frac{b}{h}=0.4}$. It can be inferred that the energy dissipation is more for a longer barrier than for a short barrier.

6 Conclusions

The phenomena of scattering of obliquely incident wave by a porous vertical barrier is studied here where the barrier is completely submerged in water of finite depth, which does not extend down to the bottom. The problem is formulated in terms of Fredholm integral equation of second kind where the unknown function represents the difference of potentials across the barrier. The integral equation is then solved using two methods: the boundary element method and the collocation method. Using the solution of the integral equation the reflection coefficient, transmission coefficient and the amount of energy dissipated are obtained which are depicted graphically by choosing certain forms of porosity distribution in the barrier. From the graph the following observations are summarised.

i) It is observed that non-uniform porosity of a barrier has significant effect on the reflection of waves and energy dissipation compared to a barrier with uniform porosity. By suitable choice of non-uniform porosity distribution in a barrier, the dissipation of the wave energy by a non-uniform porous barrier can be made larger than by a barrier with uniform porosity. This has an important bearing on reducing the wave power and thereby protecting the shore line from coastal erosion. A barrier with other choice of non-uniform porosity distribution can be designed and experimented so that the energy dissipation can be optimised.

ii) An obliquely incident wave reduces reflection and dissipation of energy as compared to the normally incident wave.

iii) Longer barrier induces more reflection and energy dissipation than a shorter barrier.

Acknowledgement This work is partially supported by SVMCM scholarship No. WBP211645525952 by Government of West Bengal, India, through Shreya Banerjee.

Competing interest The authors have no competing interests to declare that are relevant to the content of this article.

References

Banerjea S, Chakraborty R, Samanta A (2019) Boundary element approach of solving Fredholm and Volterra integral equations. Int. J. Mathematical Modelling and Numerical Optimisation, 9(1): 1-11. http://dx.doi.org/10.1504/IJMMNO.2019.10017924

Chwang AT (1983) A porous-wave maker theory.J. Fluid Mech. 132: 395-406. https://doi.org/10.1017/S0022112083001676

Gayen R, Mondal A (2014) A hypersingular integral equation approach to the porous plate problem. Applied Ocean Research,

46, 70-78. https://ui.adsabs.harvard.edu/link_gateway/2014AppOR..46...70G/doi:10.1016/j.apor.2014.01.006

Goswami SK (1983) Scattering of surface waves by a submerged fixed vertical plate in water of finite depth, J. Indian Inst. Sci., 64B, 79-88

Gupta S, Gayen R (2019) Water wave interaction with dual asymmetric non-uniform permeable plates using integral equations. Appl. Math. Comp., 346: 436-451. https://doi.org/10.1016/j.amc.2018.10.062

Losada IJ, Losada MA., Roldan A J (1992) Propagation of oblique incident waves past rigid vertical thin barriers. Applied Ocean Research, 14(3): 191-199. https://doi.org/10.1016/0141-1187(92)90014-B

Mandal BN, Chakrabarti A (2000) Water Wave Scattering by Barriers. WIT Press, Southampton, Boston

Mandal BN, Dolai DP (1994) Oblique water wave diffraction by thin verticalbarriers in water of uniform finite depth. Applied Ocean Research, 16: 195-203. https://doi.org/10.1016/0141-1187(94)90020-5

Mikhlin SG (1957) Integral Equations. Pergamon Press, New York

Mondal D, Banerjea S (2016) Scattering of water waves by an inclined porous plate submerged in ocean with ice cover. Q. Jl Mech. Appl. Math, 69: 195-213. https://doi.org/10.1093/qjmam/hbw004

Mondal D, Banerjee S, Banerjea S (2024) Effect of thin vertical porous barrier with variable permeability on an obliquely incident wave train. Wave Motion, 126: 103262. https://doi.org/10.1016/j.wavemoti.2023.103262

Parsons NF, Martin PA (1992) Scattering of water waves by submerged plates using hypersingular integral equations. Applied Ocean Research, 14: 313-321. https://doi.org/10.1016/0141-1187(92)90035-I

Parsons NF, Martin PA (1994) Scattering of water waves by submerged curved plates and by surface-piercing flat plates. Applied Ocean Research, 16: 129-139. https://doi. org/10.1016/0141-1187(94)90024-8

Porter R, Evans DV (1995) Complementary approximations to wave scattering by vertical barriers. J. Fluid Mech. 294: 155-180. https://doi.org/10.1017/S0022112095002849

Sahoo T (1998) On the scattering of water waves by porous barriers. ZAMM, 78(5): 364-370. https://doi.org/10.1002/(SICI)1521-4001(199805)78:5%3C364::AID-ZAMM364%3E3.0.CO;2-N

Samanta A, Chakraborty R, Banerjea S (2022) Line element method of solving singular integral equations. Indian J. Pure Appl. Math., 53(2): 528-541. https://doi.org/10.1007/s13226-021-00115-7

Sarkar B, De S, Roy R (2020) Oblique wave scattering by two thin non-uniform permeable vertical walls with unequal apertures in water of uniform finite depth. Waves in Rand. Complx. Med., 2021-2039. https://doi.org/10.1080/17455030.2020.1716106

Singh M, Gayen R, Kundu S (2022) Linear water wave propagation in the presence of an inclined flexible plate with variable porosity. Archive of Applied Mechanics, 92, 2593-2615. https://doi.org/10.1007/s00419-022-02201-6

Sollitt CK, Cross RH (1972) Wave transmission through permeable breakwaters. In: Proceedings of 13th Conference on Coastal Engineering 18: 27-46. https://doi.org/10.9753/icce.v13.99

Song H, Tao L (2010) An efficient scaled boundary FEM model for wave interaction with a non-uniform porous cylinder. Internat. J. for Numerical Methods in Fluids, 63: 96-118. https://doi.org/10.1002/fld.2080

Tao L, Song H, Chakrabarti S (2009) Wave interaction with a perforated circular breakwater of non-uniform porosity. J. Engng. Math, 65, 257-271. https://link.springer.com/article/10.1007/s10665-009-9287-x

Yu X (1995) Diffraction of water waves by porous breakwaters. Journal of Waterway, Port, Coastal, and Ocean Engineering. 121(6): 275-282. https://doi.org/10.1061/(ASCE)0733-950X(1995)121:6(275)